

# 1 Sources, cycling and export of nitrogen on the Greenland Ice 2 Sheet

3 \*Wadham<sup>1</sup>, J.L., J. Hawkings<sup>1</sup>, J. Telling<sup>1</sup>, D. Chandler<sup>1</sup>, J. Alcock<sup>1</sup>, E. O'Donnell<sup>2</sup>, P.  
4 Kaur<sup>1</sup>, E.A. Bagshaw<sup>1</sup>, M. Tranter<sup>1</sup>, A. Tedstone<sup>3</sup>, P. Nienow<sup>3</sup>

5 [1] – Bristol Glaciology Centre, School of Geographical Sciences, University of Bristol,  
6 University Road, BS8 1SS, UK

7 [3] - School of Geography, University of Nottingham, NG7 2RD, UK

8 [2] - School of Geoscience, University of Edinburgh, Edinburgh, EH8 9XP, UK

9

10 Correspondence to: J.L. Wadham (j.l.wadham@bris.ac.uk)

11

12

## 13 Abstract

14 Fjord and continental shelf environments in the Polar Regions are host to some of the planet's  
15 most productive ecosystems, and support economically important fisheries. Their productivity,  
16 however, is often critically dependent upon nutrient supply from upstream terrestrial  
17 environments delivered via river systems. In glacially-fed coastal ecosystems, riverine nutrients  
18 are largely sourced from melting snow and ice. The largest and most extensive glacially-fed  
19 coastal ecosystem in the Arctic is that bordering the Greenland Ice Sheet. The future primary  
20 productivity of this ecosystem, however, is uncertain. A potential increase in primary  
21 productivity driven by reduced sea ice extent and associated increased light levels may be  
22 curtailed by insufficient nutrient supply, and specifically nitrogen. Research on small valley  
23 glaciers indicates that glaciers are important sources of nitrogen to downstream environments.  
24 However, no data exists from ice sheet systems such as Greenland. Time series of nitrogen  
25 concentrations in runoff are documented from a large Greenland glacier, demonstrating  
26 seasonally elevated fluxes to the ocean. Fluxes are highest in mid-summer, when nitrogen  
27 limitation is commonly reported in coastal waters. It is estimated that approximately half of the  
28 glacially-exported nitrogen is sourced from microbial activity within glacial sediments at the

29 surface and bed of the ice sheet, doubling nitrogen fluxes in runoff. Summer dissolved inorganic  
30 nitrogen fluxes from the Greenland Ice Sheet (30-40 Gg) are a similar order of magnitude to  
31 those from a large Arctic river (Holmes et al., 2012). Nitrogen yields from the ice sheet (235 kg  
32 TDN km<sup>-2</sup> a<sup>-1</sup>), however, are approximately double those from Arctic riverine catchments. We  
33 assert that this ice sheet nitrogen subsidy to Arctic coastal ecosystems may be important for  
34 understanding coastal biodiversity, productivity and fisheries, and should be considered in future  
35 biogeochemical modelling studies of coastal marine productivity in the Arctic regions.

## 36 **1. Introduction**

37 The availability of nitrogen widely limits primary productivity in fjord (Rysgaard et al., 1999),  
38 coastal (Poulsen and Reuss, 2002;Daly et al., 1999;Nielsen and Hansen, 1999) and open ocean  
39 (Smith et al., 1985;Moore et al., 2002) waters bordering the Greenland Ice Sheet (GrIS) in  
40 summer. Hence, external sources of nitrogen to these waters, e.g. riverine runoff, may be  
41 important in sustaining the productivity of these waters and may alter in a warming climate.

42 These Greenlandic waters are some of the most productive ecosystems in the world, and boast  
43 high socio-economic value via fisheries (e.g. shrimp, halibut) (Hamilton et al., 2000). In the  
44 North Atlantic, primary productivity also draws down CO<sub>2</sub> from the atmosphere and has an  
45 important regulatory effect on global climate (Sabine et al., 2004). Warmer ocean temperatures  
46 and a lengthened growing season in the Arctic are predicted in future decades. However,  
47 increases in marine primary productivity may be capped by intensified summer nitrogen  
48 limitation (Vancoppenolle et al., 2013).

49 The GrIS discharges >1000 km<sup>3</sup> of freshwater annually to the Arctic Ocean, Irminger Sea,  
50 Labrador and Greenland Seas (Bamber et al., 2012) but has yet to be evaluated as a source of  
51 nitrogen to these waters. This freshwater flux is increasing (Bamber et al., 2012), and will  
52 continue to do so as rising air and ocean temperatures enhance rates of ice sheet melting and  
53 iceberg calving (IPCC, 2007). Greenland ice core data show the ubiquitous presence of low  
54 concentrations of dissolved inorganic nitrogen (DIN) in ice and snow, sourced from the  
55 atmosphere (Wolff, 2013). Based upon findings from small glacier systems (Hodson et al.,  
56 2008;Telling et al., 2011;Boyd et al., 2011), it is plausible that this atmospheric DIN is  
57 supplemented by nitrogen cycled into bioavailable forms by glacial biota (Telling et al.,  
58 2012;Boyd et al., 2011). While there is a mounting body of literature on nitrogen cycling on

59 valley glaciers (Telling et al., 2011;Hodson et al., 2008), there is comparatively little data on  
60 nitrogen sources and cycling on the Greenland Ice Sheet, which is likely to be important as a  
61 nutrient source to downstream fjord and marine ecosystems. High reported rates of fjord primary  
62 productivity around the GrIS margin (Jensen et al., 1999) and coastal blooms as late as  
63 July/August (Frajka-Williams and Rhines, 2010;Nielsen and Hansen, 1999) coincident with peak  
64 meltwater fluxes (Bartholomew et al., 2011) suggest that such an evaluation will be a fruitful  
65 exercise.

66 This manuscript aims to examine the sources, cycling and fluxes of nitrogen and its  
67 component species in bulk runoff exported from the GrIS during the summer melt season. We  
68 document seasonal time series of nitrogen concentrations, speciation and fluxes associated with  
69 both surface meltwaters and subglacial runoff at the large (600 km<sup>2</sup>) land-terminating Leverett  
70 Glacier (LG) in SW Greenland during the 2012 melt season. This glacier has a bedrock  
71 (Precambrian gneiss/granite (Kalsbeek, 1982)) that is consistent with large areas of the GrIS, and  
72 covers a large altitudinal range drawing meltwaters from >100 km from the ice margin. Hence,  
73 we assert that it is representative of large sectors of the Greenland margin. This manuscript  
74 builds upon recent work by (Hawkings et al., 2015), who presented a more limited dataset of  
75 dissolved inorganic subglacial nitrogen fluxes from the same catchment. We report data from a  
76 range of contextual field and experimental samples collected from sediment-laden ecosystems on  
77 and beneath the ice sheet (basal ice and incubated basal ice, glacier surface ice, snow, moulin  
78 and cryoconite waters) and subglacial incubation experiments in order to infer the relative  
79 importance of different sources of nitrogen species in runoff. Total Dissolved Nitrogen (TDN),  
80 DIN (nitrate and ammonium) and dissolved organic nitrogen (DON) were quantified in all  
81 samples and exchangeable ammonium associated with suspended sediments (SS-NH<sub>4</sub><sup>+</sup>) was  
82 analysed in runoff. These data were used to calculate seasonal nitrogen fluxes and yields from  
83 the catchment, and subsequently similar estimates for the GrIS.

84

## 85 2. Materials and Methods

### 86 2.1 Field site

87 Leverett Glacier is located on the south-west of the GrIS, approximately 300 km north of Nuuk  
88 (Figure 1.; 67.06°N, 50.10°W). The glacier overlies predominantly Precambrian gneiss/granitic  
89 bedrock, typical of much of Greenland as indicated by geological surveys of the non-glaciated  
90 areas bordering the ice sheet (Kalsbeek, 1982;Kalsbeek and Taylor, 1984). The subglacial  
91 sediments are primarily Quaternary deposits (e.g. paleosols) containing fresh organic matter that  
92 were buried during glacial advance in the last few thousands of years following the Holocene  
93 Thermal Maximum when the GrIS margin was positioned tens of kilometres further inland  
94 (Simpson et al., 2009). LG supplies runoff to the Watson River during the summer months, the  
95 largest of three glacially-fed rivers which supply Søndre Strømfjord (Figure 1). Søndre  
96 Strømfjord is the largest fjord system in western Greenland and comprises an inner fjord (up to  
97 275 m deep, 4 km wide and 80 km long) and a shallow outer fjord (<100 m deep, 1km wide and  
98 100 km long) (Nielsen et al., 2010). The inner fjord physical oceanography is influenced by  
99 meltwater, as indicated by a 50-75 m freshwater surface layer (Nielsen et al., 2010).

100

## 101 **2.2 Sample collection, processing and storage**

102 Two main sampling sites were established in summer 2012: one at the ice sheet margin (11<sup>th</sup>  
103 May – 15<sup>th</sup> July) 1km downstream of the glacier terminus (glacial runoff sampling site, Figure 1,  
104 black dot) and one on the ice sheet surface (8<sup>th</sup> May – 8<sup>th</sup> August) at a moulin located  
105 approximately 35 km from the ice margin (surface meltwater sampling site, Figure 1, red dot).

### 106 **2.2.1 Ice sheet surface sampling**

107 A field camp was established in 2012 in the mid ablation zone at LG at 1030 m elevation, 35 km  
108 from the western margin (66.97°N, 049.27°W). Here, samples of meltwater descending to the ice  
109 sheet bed (Chandler et al., 2013) were collected from the streams feeding a large moulin between  
110 5<sup>th</sup> May and 9<sup>th</sup> August (Day 129 and 222). The discharge of meltwater into this moulin was also  
111 measured (Supplementary Information 1). A range of contextual samples were collected,  
112 including ice containing dispersed cryoconite debris (referred to here as “summer ice”) and  
113 cryoconite hole waters. Cryoconite holes are water-filled cylindrical melt holes, formed by  
114 radiation heating of surface sediment and subsequent melting (Podgorny and Grenfell, 1996).  
115 The debris in the base of these holes is termed “cryoconite” which may become distributed over

116 the glacier surface during melt out of cryoconite holes in summer. Ice samples were melted in  
117 clean/sterile Whirl-pak™ bags (Nasco) overnight in a warm water bath immediately after  
118 collection (melting typically took 2-3 hrs). All meltwater samples were filtered through 47 mm,  
119 0.45 µm cellulose nitrate filters (Whatman™) in a plastic filter unit (Nalgene™ PES), pre-rinsed  
120 3 times with sample, and stored in high density polyethylene plastic bottles (Nalgene™; 30 mL).  
121 Samples were frozen immediately after filtration and only thawed out immediately prior to  
122 analysis in Bristol. Procedural blanks were processed (n=5) during the course of the sampling  
123 season, where deionised water (stored in clean plastic bottles) was treated as a sample.

## 124 **2.2.2 Bulk meltwater sampling**

125 The river draining from the subglacial portal at LG was continuously monitored during the 2012  
126 melt season (May – October) using stage measurements in a stable bedrock section ~2.2 km  
127 downstream of the terminus (Hawkings et al., 2014;Hawkings et al., 2015;Cowton et al.,  
128 2012;Tedstone et al., 2013;Hawkings et al., 2016). Stage was logged every 5-10 minutes, and  
129 converted to discharge using rhodamine dye-dilution experiments (>30 dye tracing experiments  
130 were carried out over the season using standard methods (Cowton et al., 2013)). The error in  
131 measured discharge determinations is ±10% (Tedstone et al., 2013). Suspended sediment  
132 concentrations were calculated as in previous work from bulk meltwater turbidity measurements  
133 (Cowton et al., 2012). A turbidity sensor was employed throughout the monitoring period in a  
134 similar location to stage measurements. The sensor was calibrated using manual sediment weight  
135 samples. Briefly, a recorded amount of meltwater (usually 300 mL) was filtered through a 0.45  
136 µm cellulose nitrate filter (Whatman™), oven dried overnight at 40 °C and weighed.

137

138 Bulk meltwater samples were taken approximately 1 km downstream from the LG subglacial  
139 portal, at least once a day during the main melt period (May-July). Samples were collected daily  
140 at ~10:00 hr, with occasional additional afternoon samples taken at ~18:00 hr, mostly during  
141 subglacial outburst events. A 2 L meltwater grab sample was taken in a HDPE Nalgene™ bottle  
142 (Thermo Scientific™), which had been pre-rinsed 3 times in the meltwater stream. Samples were  
143 filtered soon after collection using a Nalgene™ reusable PES filtration stack, and a 47 mm 0.45  
144 µm cellulose nitrate filter membrane (Whatman™). Filtered samples were stored in 28 mL  
145 HDPE bottles. Procedural blanks were processed (n=10) during the course of the sampling

146 season, where deionised water (stored in clean Nalgene™ HDPE plastic bottles) was treated as a  
147 sample and filtered and bottled accordingly All samples were immediately frozen and stored in  
148 the dark until analysis in Bristol.

149

### 150 **2.2.3 Basal ice sampling and incubation experiments**

151 Basal ice from the Leverett/Russell Glacier catchment was collected by chain saw from an easily  
152 accessible outcrop of debris-rich basal ice at the ice margin (within 5 km of the main LG bulk  
153 meltwater sampling site, Figure 1) by chain saw (30 x 30 x 30 cm blocks) in spring 2008 and  
154 summer 2010. The outermost ~0.5 m of ice was first removed before the blocks were cut. The  
155 blocks were wrapped in large sheets of pre-combusted foil and stored at  $\leq -20^{\circ}\text{C}$  prior to  
156 processing. Sub-samples of the ice were prepared for nitrogen analysis by chipping ~15 x 15 x 5  
157 cm chunks from the main block using a flame sterilised chisel. The outer ~10-30 mm was  
158 removed by rinsing with ultrapure ( $\geq 18.2 \text{ M}\Omega\text{cm}^{-1}$ ) deionized water, and the remaining ice was  
159 transferred into a pre-combusted glass beaker covered with foil. The ice was allowed to melt  
160 inside a laminar flow cabinet (Telstar Mini-H) at room temperature. Icemelt was filtered through  
161 Whatman polypropylene Puradisc™ 0.45  $\mu\text{m}$  syringe filters. Samples for nitrogen species  
162 determinations were stored in clean, thrice-rinsed Nalgene™ HDPE bottles. All sediment and  
163 filtered samples were stored in the dark at  $\leq -20^{\circ}\text{C}$  until analytical processing.

164

165 Long-term incubation experiments ( $> 1 \text{ yr}$ ) were conducted using sediment and meltwater  
166 derived from melted basal ice samples, in order to investigate microbially derived sources of  
167 dissolved nitrogen in a simulated subglacial environment. Three types of experiments were  
168 conducted: 1) Live control experiment with no sediment added, where the solution was  
169 meltwater from basal ice; 2) Live anaerobic experiments (sediment+meltwater from basal ice);  
170 and 3) Live aerobic experiments (sediment+meltwater from basal ice). The control sediment-free  
171 experimental nitrogen concentrations were subtracted from the live (sediment+water)  
172 experiments in order to correct for nitrogen species added from the sampling vessel and the  
173 original basal ice meltwater matrix. Hence, nitrogen concentrations reported are those that have  
174 evolved during the experiment via rock:water contact and *in situ* microbial activity.

175 Experiments were performed in the dark at 0.1 °C in modified gas-tight 500 mL  
176 borosilicate glass bottles. A sampling port towards the base of the vessel immediately above the  
177 sediment surface was used for water extraction. All incubations contained 100 mL of wet-weight  
178 sediment, 200 mL melt water and 200 mL gas headspace. Control incubation experiments  
179 contained 200 mL ice melt only. Sediment and ice melt (flushed with O<sub>2</sub>-free-N<sub>2</sub> gas) required  
180 for the anaerobic incubations were melted inside a glove-bag filled with O<sub>2</sub>-free-N<sub>2</sub> gas (BOC  
181 Ltd, UK). Meltwater/sediments were later flushed with O<sub>2</sub>-free-N<sub>2</sub> gas for >20 minutes to ensure  
182 that the sediment and water were equilibrated with an oxygen-free atmosphere. The incubations  
183 were sampled ~2 hrs after set-up (T=0 d), on day 4, 109, 190, 294, 382 and 533 and 758 (aerobic  
184 only). At each sampling point, 30 mL (15% of the initial volume) of melt water was removed,  
185 filtered through Whatman polypropylene Puradisc™ 0.45 µm syringe filters and stored at ≤ -  
186 20°C until analysis. Sampling of the anaerobic incubation experiments were conducted inside a  
187 glove-bag filled with O<sub>2</sub>-free-N<sub>2</sub> gas. All meltwater samples were frozen immediately after  
188 collection and stored frozen prior to analysis for dissolved nitrogen species.

189

## 190 **2.3 Analytical methods**

191 All meltwater samples were analysed for concentrations of total dissolved nitrogen (TDN),  
192 dissolved inorganic nitrogen (DIN, comprising nitrate and ammonium), with dissolved organic  
193 nitrogen (DON) determined by difference between TDN and DIN. Concentrations of nitrite were  
194 generally below the limit of detection and are not reported. We also analysed ammonium  
195 concentrations associated with suspended sediments in runoff (SS-NH<sub>4</sub><sup>+</sup>), where this component  
196 is assumed to be bioavailable. The nitrogen content of snow is taken from previous work  
197 conducted in the same catchment (Telling et al., 2012) and from Greenland ice cores (Wolff,  
198 2013). Pre-melt surface glacier ice nitrogen concentrations were taken from previous work  
199 conducted in **Leverett glacier catchment** (Telling et al., 2012). The detailed sampling and  
200 analytical procedures are provided in the following sections.

### 201 **2.3.1 Nitrate**

202 Nitrate was determined using a Thermo Scientific™ Dionex™ ICS-5000 ion chromatograph  
203 fitted with an IonPac™ AS11-HC-4µm anion-exchange column. A 30 mM KOH eluent

204 concentration was used, with an injection volume of 0.4  $\mu\text{L}$  and cell temperature of 35°C. The  
205 detection limit of the instrument was 0.08  $\mu\text{M N}$ . The precision of analyses, determined via  
206 analysis of eleven replicate standards at the lower end of the sample range (1.6  $\mu\text{M}$ ), was 8.1%.  
207 The accuracy of the machine was determined as -6.4%, using gravimetrically weighed standards  
208 from a 1000  $\text{mg L}^{-1}$  certified stock standard (Sigma TraceCERT®). All field nitrate data were  
209 blank corrected using field procedural blanks. The nitrate concentrations within these blanks  
210 were <0.45  $\mu\text{M}$  for surface samples and below the detection limit for runoff samples.

### 211 **2.3.2 Ammonium**

212 Ammonium was determined manually using the salicylate spectrophotometric method (Bower  
213 and Holm-Hansen, 1980; Le and Boyd, 2012), adapted for a smaller sample size (1 mL). The  
214 detection limit of the method was 0.6  $\mu\text{M N}$ . The precision of analyses was 4.9 %, calculated  
215 from five replicate standards (1.8  $\mu\text{M}$ ). Accuracy was calculated to be +0.3% (from a  
216 gravimetrically diluted certified reference standard, Sigma-Aldrich TraceCERT(R) 1000  $\text{mg L}^{-1}$ ).  
217 Ammonium concentrations in field samples were blank corrected using field procedural blanks,  
218 and were all above the limit of detection. Mean blank correction factors for ammonium were  
219 0.75  $\mu\text{M N}$  for surface samples. Runoff blank corrections were below the detection limit of the  
220 instrument.

### 221 **2.3.3 Total Dissolved Nitrogen (TDN)**

222 Total Nitrogen was determined on most runoff samples using a Lachat QuikChem® 8500 Flow  
223 Injection Analyser system, with digestion unit (method number 10-107-04-3-E). The detection  
224 limit of the instrument was 1.4  $\mu\text{M TDN}$ , the precision of analyses was calculated as 11.3% from  
225 six 3.6  $\mu\text{M}$  replicate reference standards (gravimetrically diluted from a certified reference  
226 standard, Sigma-Aldrich TraceCERT(R) 1000  $\text{mg L}^{-1}$ ). Accuracy was determined using the same  
227 reference standards as -0.4%. All TDN data were field blank corrected (2  $\mu\text{M}$  for surface  
228 samples, and no correction for runoff samples since these were below the detection limit of the  
229 instrument).

230

### 231 **2.3.4 Exchangeable $\text{NH}_4^+$ in suspended sediment ( $\text{SS-NH}_4^+$ ).**



232 Measurements were conducted using the method described by (Maynard et al., 2007). Filters  
233 containing suspended solids were placed into polypropylene centrifuge tubes and the  $\text{NH}_4^+$  was  
234 then extracted with 10 ml of 2M KCl for 30 minutes on an automatic shaking table (160 rpm).  
235 Extracts were decanted into additional centrifuge tubes, centrifuged at 4500 rpm for 5 min, and  
236 filtered through 0.45  $\mu\text{m}$  inline Whatman® polypropylene Puradisc filters. When immediate  
237 analysis was not possible, they were immediately, frozen ( $-20^\circ\text{C}$ ) until analysis. A second  
238 sequential extraction was then performed to extract any residual sediment bound  $\text{NH}_4^+$ . Extracts  
239 were analyzed on a Bran and Luebbe Autoanalyzer 3, with a detection limit in extracts of 0.9  $\mu\text{M}$   
240 N, equivalent to 0.09  $\mu\text{M}$  N for a typical sediment mass of 0.1 g. The  $\text{NH}_4^+$  concentrations from  
241 the first and second extracts were combined to give a total  $\text{NH}_4^+$  for the suspended sediment  
242 samples. Dry weights for sediment samples were obtained by washing residual sediment from  
243 filters into centrifuge tubes with MQ water, centrifuging at 4500 rpm for 5 min, then repeating  
244 with a further MQ wash and centrifuging stage to remove any residual KCl. Sediments were then  
245 oven dried (overnight at  $40^\circ\text{C}$ ) and weighed. This gave concentrations of exchangeable  $\text{NH}_4^+$  of  
246  $\mu\text{g N g}^{-1}$ , which were converted into units of  $\mu\text{M N g}^{-1}$  and then to  $\mu\text{M N}$  by multiplying by the  
247 instantaneous suspended sediment concentration (in  $\text{g L}^{-1}$ ) at the time of sample collection. SS-  
248  $\text{NH}_4^+$  fluxes ( $\mu\text{M N s}^{-1}$ ) were subsequently calculated from the product of the  $\text{NH}_4^+$  concentration  
249 and bulk discharge (in L) at the time of sample collection.

250

## 251 **2.4 Flux calculations**

### 252 **2.4.1 Nitrogen fluxes from Leverett Glacier**

253 Nitrogen fluxes over the entire melt season (May - September) are calculated for LG for the 2012  
254 melt season, which was a record melt year in Greenland (Tedesco et al., 2013). Discharge  
255 weighted mean concentrations of dissolved nitrogen species and SS- $\text{NH}_4^+$  for LG runoff were  
256 calculated for the 2012 melt season. Use of discharge weighted mean (DWM) concentrations  
257 lowers the mean nitrogen concentrations in bulk meltwaters, since high discharge values are  
258 generally accompanied by low nitrogen concentrations. Hence, this method provides a more  
259 conservative estimate of nitrogen fluxes. We use minimum and maximum concentrations of  
260 nitrogen species to illustrate the potential maximum range of nitrogen fluxes under different  
261 hydro-climatological regimes. The product of the DWM, minimum and maximum concentration

262 of each nitrogen species and the runoff flux for the summer discharge monitoring period in 2012  
263 from LG (2.2 km<sup>3</sup>, Supplementary Figure 5) generated the total seasonal fluxes of these nitrogen  
264 species. We did not measure the particulate organic nitrogen (PON) concentrations in runoff, and  
265 in previous years these concentrations have been below the detection limit of standard analytical  
266 methods. However, we did calculate the SS-NH<sub>4</sub><sup>+</sup> fluxes in the same manner as the dissolved  
267 nitrogen species. Total fluxes of dissolved and SS-NH<sub>4</sub><sup>+</sup> in LG runoff during the 2012 melt  
268 season are presented in Table 2. Errors on these estimates due to discharge uncertainty and  
269 catchment area are of the order of ±10% and ±25% respectively (Tedstone et al., 2013; Cowton et  
270 al., 2012), giving a combined uncertainty of ±27%.

#### 271 **2.4.2 Nitrogen fluxes from the Greenland Ice Sheet**

272 Currently, there are no other seasonal time series of nitrogen concentrations in runoff from large  
273 Greenland outlet glaciers. Hence, nitrogen concentrations in LG runoff are used in order to  
274 generate order of magnitude flux estimates for nitrogen associated with Greenland freshwater  
275 export. We base our calculations upon the premise that LG is representative of large areas of the  
276 GrIS, for several reasons. First, LG displays a high altitudinal range (250 – 1510 m a.s.l.) and  
277 extends for > 80 km inland, like many large Greenland outlets. Hence, nitrogen supply from  
278 snow and ice melt are likely to be representative of other large catchments draining the ice sheet.  
279 Second, microbial processes (e.g. nitrogen fixation, nitrification, organic matter mineralisation),  
280 which are thought to generate approximately half of the ice sheet nitrogen in runoff (via DON,  
281 nitrate and ammonium), are reported from a wide range of other glacial systems worldwide  
282 including the Greenland Ice Sheet (Hodson et al., 2005; Boyd et al., 2011; Telling et al., 2012), a  
283 reflection of the ubiquitous nature of microbial ecosystems upon glacier surfaces and at glacier  
284 beds. Third, the bedrock geology at LG is representative of large areas of the GrIS (see Section  
285 2.1). This suggests that the drivers for nitrogen export at Leverett Glacier are likely to be  
286 applicable to other large catchments, which account for the bulk of the freshwater flux from the  
287 ice sheet to the oceans. Our approach is widely employed for calculating solute fluxes from ice  
288 sheet systems where datasets are sparse due to the difficulty of making measurements (Wadham  
289 et al., 2010; Bhatia et al., 2013; Lawson et al., 2013; Hawkings et al., 2014; Hawkings et al., 2016).

290 Fluxes of nitrogen from the GrIS are calculated from the product of DWM, minimum and  
291 maximum concentrations of the different nitrogen species at LG glacier (Table 3) and the total

292 ice sheet runoff flux for 2012 and the mean runoff flux of 2000-2011 (Tedesco et al., 2013)  
293 (Table 3). The latter is modelled using the MAR regional climate model. Errors for meltwater  
294 runoff determinations via the MAR model are estimated 10% (Vernon et al., 2013). Hence, we  
295 might expect similar uncertainty to propagate to nutrient flux determinations. We also estimate  
296 the potential nitrogen fluxes exported to the ocean by iceberg calving, which have a potential far-  
297 field influence within the open ocean (Syvitski et al., 2001;Smith Jr. et al., 2013). Iceberg  
298 nitrogen fluxes are taken to be the product of the iceberg freshwater flux and mean nitrogen  
299 concentrations in Greenland ice cores (Table 3). We employ a freshwater flux for Greenland  
300 icebergs of  $600 \text{ km}^3 \text{ a}^{-1}$ , based upon approximate average values for the last decade (Bamber et  
301 al., 2012). We assume that the mean concentrations of nitrogen in icebergs are similar to those  
302 reported in Greenland ice cores (Wolff, 2013), which are also in line with those reported in LG  
303 catchment (Telling et al., 2012). This is a conservative estimate, since additional nitrogen supply  
304 is likely associated with sediments entombed within icebergs. Results from this work indicate  
305 that the SS-NH<sub>4</sub> content of ice containing even trace amounts of debris may display elevated  
306 nitrogen concentrations which are five times higher than in ice with no debris (Table 1).

307

308

### 309 **3. Results and Discussion**

#### 310 **3.1 Sources of nitrogen in runoff**

311 The LG runoff time series demonstrates that the GrIS provides a continuous supply of nitrogen  
312 to downstream ecosystems throughout the main melt period (Figure 2). Concentrations of TDN  
313 are significant (1-10 $\mu\text{M}$ ) and mean nitrate concentrations (1.8  $\mu\text{M}$ ) alone are higher than those  
314 reported in surface ocean and fjord waters (<0.1-1 $\mu\text{M}$ ) in western Greenland in summer (Nielsen  
315 and Hansen, 1999;Arendt et al., 2010;Hopwood et al., 2016). Higher concentrations of nitrate are  
316 observed in deeper ocean waters, but upward diffusion and advection are often limited by a  
317 stratified water column during the summer months (Arendt et al., 2010). DIN, which is readily  
318 available to marine phytoplankton, accounts for half of the TDN in LG runoff, supplemented by  
319 SS-NH<sub>4</sub><sup>+</sup> from the ice sheet bed. A component (~50%) of the DIN measured in LG runoff  
320 originates from natural and anthropogenic atmospheric sources, via melting of snow and ice

321 (Wolff, 2013) (Table 1). LG drains a large catchment (active hydrological catchment area = 600  
322 km<sup>2</sup> ±25% (Cowton et al., 2012)) with a high altitudinal range (extending to >1500 m a.s.l.).  
323 New moulins open up and surface lakes drain with snow line retreat (Bartholomew et al., 2011),  
324 providing a mechanism by which new sources of DIN are fed to runoff. Water fluxes control the  
325 overall nitrogen flux, which rises through summer to attain high values during the sampling  
326 period in mid-July (Figure 2). The bulk runoff chemical sampling record did not extend beyond  
327 this point. However, we assert that runoff nitrogen fluxes will continue to be high in late  
328 July/early August, as evidenced by the sustained high fluxes of nitrogen species in moulin waters  
329 up until 9<sup>th</sup> August (Day 222, Suppl. Figure 5). This is significant given the reported nitrogen  
330 limitation of fjord and marine phytoplankton in mid-summer, once the water column becomes  
331 more stratified and deep marine sources of nitrogen become more inaccessible (Rysgaard et al.,  
332 1999; Budeus and Schneider, 1995).

333 A striking feature of the runoff dataset is the factor of four increase in concentrations of  
334 TDN in LG runoff (4.5 µM, 5.7 µM including SS-NH<sub>4</sub><sup>+</sup>) compared with those in snow and ice  
335 (<1 µM), reflecting enhancements in dissolved organic nitrogen, ammonium and nitrate (Figure  
336 3, Table 1). Similar findings have been reported at small valley glaciers (Hodson et al., 2008),  
337 and imply the acquisition of significant quantities of nitrogen within the glacier. A substantial  
338 proportion of this enhancement must occur in sedimentary environments at the ice sheet bed, as  
339 indicated by a significant association between TDN in moulin waters and bulk runoff, but a  
340 positive intercept of 2.5 µM (Figure 4). A range of possible sources exist for this additional  
341 nitrogen in runoff. Our wider contextual survey of the nitrogen content of basal and surface ice  
342 and meltwaters and subglacial incubation experiments allows us to conjecture on these sources.  
343 For nitrate, enhancement is likely to occur in the subglacial environment, since nitrate  
344 concentrations in moulin waters and snow/ice are similar (Table 1). The basal regions of ice  
345 sheets are viable habitats for microbial life and previous work has demonstrated the activity of  
346 nitrifying bacteria, which transform ammonium to nitrate, at small Alpine valley glaciers (Boyd  
347 et al., 2011; Wynn et al., 2007) and Subglacial Lake Whillans in Antarctica (Christner et al.,  
348 2014). In support of this, long-term incubation experiments using LG subglacial sediments  
349 (Figure 5) show the release of up to 5 µM nitrate under aerobic conditions in live sediments and  
350 an absence of this production in live controls (no sediment) and under anaerobic conditions. The

351 simultaneous removal of ammonium ions is consistent with nitrification as the source of this  
352 nitrate, likely in more aerobic subglacial channel-marginal sedimentary environments.

353 The enhancement of DON concentrations in moulin waters relative to snow and ice, and  
354 in runoff relative to moulin waters is also significant (independent t-test,  $p=0.05$ ) and suggests  
355 the acquisition of DON in surface and basal ecosystems respectively. This is consistent with  
356 previous work that has suggested the presence of a significant nitrogen-rich component to  
357 dissolved organic matter exported from glacier ecosystems in runoff (Hood et al., 2009; Lawson  
358 et al., 2014; Bhatia et al., 2013). Likely surface sources are cryoconite holes and debris-rich ice,  
359 which display elevated DON concentrations relative to pre-melt ice and snow (Figure 2, Table  
360 1). These debris-laden environments support diverse microbial communities, which actively fix  
361 carbon dioxide from the atmosphere (Stibal et al., 2012). We assert that mineralization of organic  
362 matter in such environments generates the elevated DON concentrations in surface waters by  
363 microbial activity or by leaching from allochthonous organic matter in debris. The factor of two  
364 enhancement in DON concentrations in runoff relative to moulin waters reflects an even greater  
365 subglacial input of these nitrogen species. It is notable also that, while ammonium concentrations  
366 in bulk runoff are generally low ( $<$  detection limit at  $0.6 \mu\text{M}$ ), both DON and ammonium  
367 concentrations in runoff are often elevated during subglacial outburst events, rising to up to 3 and  
368  $6 \mu\text{M}$  respectively (Figures 2 and 6). These events are known to expel long-term stored  
369 meltwaters and sediments from beneath the ice sheet in response to surface lakes drainage  
370 (Bartholomew et al., 2011). A subglacial source of these waters is clearly evident from elevated  
371 sulphate concentrations, which rise during outburst events. Sulphate ions are uniquely generated  
372 in inefficient distributed drainage pathways at the glacier bed, where comminution of the  
373 underlying bedrock releases highly reactive iron sulphide minerals to meltwaters. These oxidise  
374 rapidly to give sulphate (Tranter et al., 1993). The elevated runoff DON and ammonium during  
375 such events implies a source in subglacial sedimentary ecosystems. Long-term incubation  
376 experiments presented in Figure 5 strongly support a subglacial source for DON but do not show  
377 elevated concentrations of ammonium in live experiments. We propose that the subglacial  
378 acquisition of DON reflects *in situ* microbial activity, as reported beneath smaller valley glaciers  
379 (Hodson et al., 2005). The low dissolved organic carbon (DOC):DON ratio in runoff (mean=9.5,  
380 DOC data from (Hawkings, 2015)) is similar to other world glaciers (Hood and Scott, 2008) and  
381 is consistent with a microbial source for DON. It contrasts with the higher mean DOC:DON

382 ratios for Arctic rivers (mean=48) which include a greater terrestrial contribution (Lobbés et al.,  
383 2000). These findings support the notion that dissolved organic matter exported from the GrIS  
384 may be highly bioavailable to marine bacteria (Lawson et al., 2014; Lawson et al., 2013; Bhatia et  
385 al., 2010), as has been suggested for glacier systems elsewhere (Hood et al., 2009).

386 The subglacial source of the enhanced ammonium concentrations in long-term stored  
387 subglacial waters released during outburst events is less clear. Ammonium concentrations in  
388 basal ice and outburst waters were relatively high (mean = 2-3  $\mu\text{M}$ ) (Table 1; Figure 6) but our  
389 subglacial incubation experiments time series showed no significant enhancement of ammonium  
390 from initial concentrations over time (Figure 5). Enhancement of ammonium concentrations in  
391 long-term stored subglacial meltwaters have been documented previously in Antarctic Subglacial  
392 Lake Whillans, inferred to reflect microbial mineralisation (Christner et al., 2014). There are  
393 several potential reasons for the static ammonium concentrations during our laboratory  
394 experiments. It may reflect the difficulty of replicating microbial processes under laboratory  
395 conditions, together with elevated starting ammonium concentrations at  $t=0$  in experiments  
396 (basal ice mean  $\text{NH}_4^+=2.7 \mu\text{M}$ ). Second, it may indicate that the subglacial process that generates  
397 ammonium ions is not modelled well by laboratory experiments. For example, ammonium may  
398 be released to solution directly or indirectly by crushing of the underlying bedrock (Dixon et al.,  
399 2012), as occurs for other species such as hydrogen (Telling et al., 2015). Greenland gneiss  
400 contains very small concentrations of nitrogen ( $9 \mu\text{g N g}^{-1}$  (Holloway and Dahlgren, 2002)), but  
401 glacial crushing and release of this nitrogen from bedrock as ammonium has the potential to  
402 generate concentrations an order of magnitude higher concentrations of ammonium than those  
403 observed in incubation experiments. Overall, data presented here suggests the operation of a  
404 suite of diverse mechanisms that supply nitrogen species from snow and icemelt, enhancing them  
405 in supra- and subglacial ecosystems prior to meltwaters being evacuated at the ice margin. This  
406 is consistent with recent work in Alpine regions that clearly demonstrated the potential for  
407 glacier-fed catchments to display enhanced nitrogen concentrations in runoff relative to  
408 snowmelt-fed systems (Saros et al., 2010).

### 409 3.2 Fluxes of nitrogen from Leverett Glacier

410 Total dissolved nitrogen (including SS- $\text{NH}_4^+$ ) fluxes from LG in summer are on average  $0.14 \text{ t a}^{-1}$   
411 (Table 2). The estimated TDN yields for the Leverett Glacier catchment arising from this flux

412 are  $236 \text{ kg km}^{-2}$  ( $164 \text{ kg m}^{-2}$  excluding  $\text{SS-NH}_4^+$ ), which is an order of magnitude higher than the  
413 typical annual TDN yields measured in large Arctic rivers ( $36\text{-}81 \text{ kg km}^{-2}$ ) (Holmes et al., 2012).  
414 This high yield largely arises from the high specific water yield at LG ( $3.7 \times 10^6 \text{ m}^3 \text{ km}^{-2} \text{ a}^{-1}$ ), in  
415 comparison to the water yield (July-October) of the largest Arctic rivers, which is two orders of  
416 magnitude lower ( $9.3 \times 10^4 \text{ m}^3 \text{ km}^{-2} \text{ a}^{-1}$ , calculated from a water flux for the six largest Arctic  
417 rivers of  $1011 \text{ km}^3 \text{ a}^{-1}$  from July to October and a gauged catchment area of  $10.9 \times 10^6 \text{ km}^2$ )  
418 (Holmes et al., 2012). This implies that there is a much higher continuous flux of dissolved  
419 nitrogen species per unit area from the ice sheet in summer than from high Arctic River  
420 catchments, reflecting the acquisition of dissolved N species from both melting snow and ice on  
421 the surface and sedimentary environments at the ice sheet bed.

### 422 **3.3 Fluxes of nitrogen from the Greenland Ice Sheet**

423 The estimated summer mid-range TN flux (including  $\text{SS-NH}_4^+$ ) from the GrIS is  $\sim 27 \text{ Gg}$  (2000-  
424 2011) and  $43 \text{ Gg}$  (2012) (Table 3) using discharge weighted mean concentrations, with potential  
425 flux ranges of 7-86 and 11-137 for 2000-2010 and 2012 respectively. The mean values are of a  
426 similar order of magnitude to a large Arctic river (the average TDN flux for the Lena, Yenisey,  
427 Ob Rivers, July-October is  $41 \text{ Gg}$  (Holmes et al., 2012)). The glacial nitrogen fluxes largely  
428 supply different ocean basins to the Arctic rivers (Bamber et al., 2012; Holmes et al., 2012). We  
429 contend that ice sheet derived nitrogen fluxes are likely to rise with enhanced melting in a  
430 warmer climate and could, therefore, stimulate increased primary production in downstream  
431 coastal ecosystems. Evidence from a single melt year suggests that within-season fluxes of  
432 nitrogen species rise exponentially with increasing glacial water fluxes (Figure 2). The degree of  
433 future nitrogen flux increase in warm melt years, however, is difficult to predict. The  
434 atmospheric nitrogen flux (largely as DIN) are likely to scale with increasing melt volumes as  
435 has been suggested else (Hawkings et al., 2015). However, the magnitude of increase will  
436 depend upon the availability of glacial ice and snow from post-industrial times, since these  
437 display elevated atmospheric DIN compared with pre-industrial ice (Olivier et al., 2006). DON  
438 and non-atmospheric ammonium fluxes might also be expected to increase as the zone of melting  
439 expands and there is more extensive contact of meltwater with organic matter in surface and  
440 subglacial ecosystems.

441           The impact of present and future nitrogen fluxes upon fjord and coastal marine  
442 ecosystems around Greenland is unknown, and requires further study. The input of nutrients  
443 associated with Greenland icebergs and runoff may sustain elevated primary productivity beyond  
444 the spring phytoplankton bloom, and offers one possible explanation for the reported mid-  
445 summer phytoplankton bloom in Western Greenland (Frajka-Williams and Rhines, 2010;Nielsen  
446 and Hansen, 1999). Nitrogen limitation is common in fjord and coastal waters in summer, and  
447 hence any increase in DIN supply has the potential to enhance primary productivity.

448

#### 449 **4 Conclusions**

450 In summary, our findings at Leverett Glacier suggest that large glacial outlet glaciers draining  
451 the Greenland Ice Sheet provide a continuous source of dissolved nitrogen in runoff through the  
452 summer months, a proportion of which is likely to originate from microbial ecosystems on and  
453 beneath the ice. The degree to which these nitrogen fluxes are modified by proglacial processes  
454 is unknown, as are the potential impacts upon fjord and coastal marine biological productivity.  
455 However, phytoplankton in coastal Greenlandic waters often become limited by nitrogen  
456 availability by mid-summer, when the glacial nitrogen flux to coastal waters is highest. TDN  
457 yields from Leverett Glacier are an order of magnitude higher than those reported for Arctic  
458 rivers, a reflection of the high surface melt rates (and hence water fluxes) and continuous  
459 nitrogen supply from several sources within the ice sheet. Estimated fluxes of nitrogen from the  
460 ice sheet are similar in magnitude to those of a large Arctic river. Our findings suggest that a  
461 melting GrIS may be an important source of nitrogen to downstream coastal ecosystems, and that  
462 these nitrogen fluxes are likely to increase in a warming climate.

463

464

465

466

467



468

469

470

## 471 **5 References**

472 Arendt, K. E., Nielsen, T. G., Rysgaard, S., and Tonnesson, K.: Differences in plankton  
473 community structure along the Godthabsfjord, from the Greenland Ice Sheet to offshore waters,  
474 *Mar Ecol Prog Ser*, 401, 49-62, Doi 10.3354/Meps08368, 2010.

475 Bamber, J., van den Broeke, M., Ettema, J., Lenaerts, J., and Rignot, E.: Recent large increases  
476 in freshwater fluxes from Greenland into the North Atlantic, *Geophys Res Lett*, 39, Artn L19501  
477 Doi 10.1029/2012gl052552, 2012.

478 Bartholomew, I., Nienow, P., Sole, A., Mair, D., Cowton, T., Palmer, S., and Wadham, J.:  
479 Supraglacial forcing of subglacial drainage in the ablation zone of the Greenland ice sheet,  
480 *Geophys. Res. Lett.*, 38, L08502, 10.1029/2011gl047063, 2011.

481 Bhatia, M. P., Das, S. B., Longnecker, K., Charette, M. A., and Kujawinski, E. B.: Molecular  
482 characterization of dissolved organic matter associated with the Greenland ice sheet, *Geochim*  
483 *Cosmochim Ac*, 74, 3768-3784, DOI 10.1016/j.gca.2010.03.035, 2010.

484 Bhatia, M. P., Das, S. B., Xu, L., Charette, M. A., Wadham, J. L., and Kujawinski, E. B.:  
485 Organic carbon export from the Greenland ice sheet, *Geochim Cosmochim Ac*, 109, 329-344,  
486 DOI 10.1016/j.gca.2013.02.006, 2013.

487 Bower, C. E., and Holm-Hansen, T.: A Salicylate–Hypochlorite Method for Determining  
488 Ammonia in Seawater, *Can J Fish Aquat Sci*, 37, 794-798, 10.1139/f80-106, 1980.

489 Boyd, E. S., Lange, R. K., Mitchell, A. C., Havig, J. R., Hamilton, T. L., Lafreniere, M. J.,  
490 Shock, E. L., Peters, J. W., and Skidmore, M.: Diversity, Abundance, and Potential Activity of  
491 Nitrifying and Nitrate-Reducing Microbial Assemblages in a Subglacial Ecosystem, *Appl*  
492 *Environ Microb*, 77, 4778-4787, Doi 10.1128/Aem.00376-11, 2011.

493 Budeus, G., and Schneider, W.: On the Hydrography of the Northeast Water Polynya, *J Geophys*  
494 *Res-Oceans*, 100, 4287-4299, Doi 10.1029/94jc02024, 1995.

495 Chandler, D. M., Wadham, J. L., Lis, G. P., Cowton, T., Sole, A., Bartholomew, I., Telling, J.,  
496 Nienow, P., Bagshaw, E. B., Mair, D., Vinen, S., and Hubbard, A.: Evolution of the subglacial  
497 drainage system beneath the Greenland Ice Sheet revealed by tracers, *Nat Geosci*, 6, 195-198,  
498 Doi 10.1038/Ngeo1737, 2013.

499 Christner, B. C., Priscu, J. C., Achberger, A. M., Barbante, C., Carter, S. P., Christianson, K.,  
500 Michaud, A. B., Mikucki, J. A., Mitchell, A. C., Skidmore, M. L., Vick-Majors, T. J., and the,

501 W. S. T.: A microbial ecosystem beneath the West Antarctic ice sheet, *Nature*, 512, 310-313,  
502 10.1038/nature13667

503 <http://www.nature.com/nature/journal/v512/n7514/abs/nature13667.html> - supplementary-  
504 [information](#), 2014.

505 Cowton, T., Nienow, P., Bartholomew, I., Sole, A., and Mair, D.: Rapid erosion beneath the  
506 Greenland ice sheet, *Geology*, 40, 343-346, 10.1130/g32687.1, 2012.

507 Cowton, T., Nienow, P., Sole, A., Wadham, J., Lis, G., Bartholomew, I., Mair, D., and Chandler,  
508 D.: Evolution of drainage system morphology at a land-terminating Greenlandic outlet glacier, *J*  
509 *Geophys Res-Earth*, 118, 29-41, Doi 10.1029/2012jf002540, 2013.

510 Daly, K. L., Wallace, D. W. R., Smith, W. O., Skoog, A., Lara, R., Gosselin, M., Falck, E., and  
511 Yager, P. L.: Non-Redfield carbon and nitrogen cycling in the Arctic: Effects of ecosystem  
512 structure and dynamics, *J Geophys Res-Oceans*, 104, 3185-3199, Doi 10.1029/1998jc900071,  
513 1999.

514 Dixon, J. C., Campbell, S. W., and Durham, B.: Geologic nitrogen and climate change in the  
515 geochemical budget of Kärkevagge, Swedish Lapland, *Geomorphology*, 167-168, 70-76,  
516 <http://dx.doi.org/10.1016/j.geomorph.2012.03.011>, 2012.

517 Frajka-Williams, E., and Rhines, P. B.: Physical controls and interannual variability of the  
518 Labrador Sea spring phytoplankton bloom in distinct regions, *Deep-Sea Res Pt I*, 57, 541-552,  
519 DOI 10.1016/j.dsr.2010.01.003, 2010.

520 Hamilton, L., Lyster, P., and Otterstad, O.: Social Change, Ecology and Climate in 20th-Century  
521 Greenland, *Climatic Change*, 47, 193-211, 10.1023/a:1005607426021, 2000.

522 Hawkings, J., Wadham, J. L., Tranter, M., Raiswell, R., Benning, L. G., Statham, P. J., Tedstone,  
523 A., and Nienow, P.: Ice sheets as a significant source of highly reactive nanoparticulate iron to  
524 the oceans, *Nature Communications*, 5, doi:10.1038/ncomms4929, 2014.

525 Hawkings, J.: An investigation into the production and export of nutrients from glaciers PhD,  
526 School of Geographical Sciences, University of Bristol, bristol, 241 pp., 2015.

527 Hawkings, J., Wadham, J. L., Tranter, M., Telling, J., Bagshaw, E. A., Beaton, A., Simmons, S.  
528 L., Tedstone, A., and Nienow, P. W.: The Greenland Ice Sheet as a hot spot of phosphorus  
529 weathering and export in the Arctic, *Global Biogeochem Cy*, 30, 191-210, 2016.

530 Hawkings, J. R., Wadham, J. L., Tranter, M., Lawson, E., Sole, A., Cowton, T., Tedstone, A. J.,  
531 Bartholomew, I., Nienow, P., Chandler, D., and Telling, J.: The effect of warming climate on  
532 nutrient and solute export from the Greenland Ice Sheet, *Geochemical Perspectives Letters*, 1,  
533 94-104, <http://dx.doi.org/10.7185/geochemlet.1510>, 2015.

534 Hodson, A., Anesio, A. M., Tranter, M., Fountain, A., Osborn, M., Priscu, J., Laybourn-Parry, J.,  
535 and Sattler, B.: Glacial ecosystems, *Ecol Monogr*, 78, 41-67, 2008.

536 Hodson, A. J., Mumford, P. N., Kohler, J., and Wynn, P. M.: The High Arctic glacial ecosystem:  
537 new insights from nutrient budgets, *Biogeochemistry*, 72, 233-256, DOI 10.1007/s10533-004-  
538 0362-0, 2005.

539 Holloway, J. M., and Dahlgren, R. A.: Nitrogen in rock: Occurrences and biogeochemical  
540 implications, *Global Biogeochem Cy*, 16, 10.1029/2002GB001862, 2002.

541 Holmes, R. M., McClelland, J. W., Peterson, B. J., Tank, S. E., Bulygina, E., Eglinton, T. I.,  
542 Gordeev, V. V., Gurtovaya, T. Y., Raymond, P. A., Repeta, D. J., Staples, R., Striegl, R. G.,  
543 Zhulidov, A. V., and Zimov, S. A.: Seasonal and Annual Fluxes of Nutrients and Organic Matter  
544 from Large Rivers to the Arctic Ocean and Surrounding Seas, *Estuar Coast*, 35, 369-382, DOI  
545 10.1007/s12237-011-9386-6, 2012.

546 Hood, E., and Scott, D.: Riverine organic matter and nutrients in southeast Alaska affected by  
547 glacial coverage, *Nat Geosci*, 1, 583-587, Doi 10.1038/Ngeo280, 2008.

548 Hood, E., Fellman, J., Spencer, R. G. M., Hernes, P. J., Edwards, R., D'Amore, D., and Scott, D.:  
549 Glaciers as a source of ancient and labile organic matter to the marine environment, *Nature*, 462,  
550 1044-U1100, Doi 10.1038/Nature08580, 2009.

551 Hopwood, M. J., Connelly, D. P., Arendt, K. E., Juul-Pedersen, T., Stinchcombe, M., Meire, L.,  
552 Esposito, M., and Krishna, R.: Seasonal changes in Fe along a glaciated Greenlandic fjord,  
553 *Frontiers in Earth Science*, 4, 10.3389/feart.2016.00015, 2016.

554 IPCC: in: *Climate Change 2007: The Physical Science Basis. Contribution of Working Group I*  
555 *to the Fourth Assessment Report of the Intergovernmental Panel on Climate Change*, edited by:  
556 Solomon, S., Qin, D., Manning, M., Chen, Z., Marquis, M., Averyt, K. B., Tignor, M., and  
557 Miller, H. L., Cambridge University Press, , Cambridge, United Kingdom and New York, NY,  
558 USA, 2007., 2007.

559 Jensen, H. M., Pedersen, L., Burmeister, A., and Hansen, B. W.: Pelagic primary production  
560 during summer along 65 to 72 degrees N off West Greenland, *Polar Biology*, 21, 269-278, DOI  
561 10.1007/s003000050362, 1999.

562 Kalsbeek, F.: The evolution of the Precambrian shield of Greenland, *Geol. Rundsch*, 71, 38-60,  
563 1982.

564 Kalsbeek, F., and Taylor, P. N.: Pb-isotopic studies of proterozoic igneous rocks, west  
565 Greenland, with implications on the evolution of the Greenland shield, in: *The deep Proterozoic*  
566 *crust in the North Atlantic Provinces*, NATO ASI Series, Series C, Mathematical and Physical  
567 Sciences, D. Reidal Publishing Company, 1984.

568 Lawson, E., Wadham, J. L., Tranter, M., Stibal, M., Lis, G., Butler, C., Laybourn-Parry, J.,  
569 Nienow, P., Chandler, D., and Dewsbury, P.: Greenland Ice Sheets exports labile organic carbon  
570 to the Arctic oceans, *Biogeosciences Discussions*, 10, 19311–19345, 2013.

571 Lawson, E. C., Bhatia, M. P., Wadham, J. L., and Kujawinski, E. B.: Continuous Summer Export  
572 of Nitrogen-Rich Organic Matter from the Greenland Ice Sheet Inferred by Ultrahigh Resolution  
573 Mass Spectrometry, *Environ Sci Technol*, 48, 14248-14257, 10.1021/es501732h, 2014.

574 Le, P. T. T., and Boyd, C. E.: Comparison of Phenate and Salicylate Methods for Determination  
575 of Total Ammonia Nitrogen in Freshwater and Saline Water, *Journal of the World Aquaculture  
576 Society*, 43, 885-889, 10.1111/j.1749-7345.2012.00616.x, 2012.

577 Lobbes, J. M., Fitznar, H. P., and Kattner, G.: Biogeochemical characteristics of dissolved and  
578 particulate organic matter in Russian rivers entering the Arctic Ocean, *Geochim Cosmochim Acta*,  
579 64, 2973-2983, Doi 10.1016/S0016-7037(00)00409-9, 2000.

580 Maynard, D. G., Kalra, Y. P., and Crumgaugh, J. A.: Nitrate and exchangeable ammonium  
581 nitrogen, in: *Soil Sampling and Methods of Analysis*, edited by: Carter, M. R., and Gregorich, E.  
582 G., CRC Press, Boca Raton, Fla, 2007.

583 Moore, J. K., Doney, S. C., Glover, D. M., and Fung, I. Y.: Iron cycling and nutrient-limitation  
584 patterns in surface waters of the World Ocean, *Deep-Sea Res Pt II*, 49, 463-507, 2002.

585 Nielsen, M. H., Erbs-Hansen, D. R., and Knudsen, K. L.: Water masses in Kangerlussuaq, a  
586 large fjord in West Greenland: the processes of formation and the associated foraminiferal fauna,  
587 *Polar Res*, 29, 159-175, DOI 10.1111/j.1751-8369.2010.00147.x, 2010.

588 Nielsen, T. G., and Hansen, B. W.: Plankton community structure and carbon cycling on the  
589 western coast of Greenland during the stratified summer situation. I. Hydrography,  
590 phytoplankton and bacterioplankton, *Aquat Microb Ecol*, 16, 205-216, Doi 10.3354/Ame016205,  
591 1999.

592 Olivier, S., Blaser, C., Brutsch, S., Frolova, N., Gaggeler, H. W., Henderson, K. A., Palmer, A.  
593 S., Papina, T., and Schwikowski, M.: Temporal variations of mineral dust, biogenic tracers, and  
594 anthropogenic species during the past two centuries from Belukha ice core, Siberian Altai, *J  
595 Geophys Res-Atmos*, 111, Artn D05309  
596 Doi 10.1029/2005jd005830, 2006.

597 Podgorny, I. A., and Grenfell, T. C.: Absorption of solar energy in a cryoconite hole, *Geophys  
598 Res Lett*, 23, 2465-2468, 10.1029/96GL02229, 1996.

599 Poulsen, L. K., and Reuss, N.: The plankton community on Sukkertop and Fylla Banks off West  
600 Greenland during a spring bloom and post-bloom period: Hydrography, phytoplankton and  
601 protozooplankton, *Ophelia*, 56, 69-85, 2002.

602 Rysgaard, S., Nielsen, T. G., and Hansen, B. W.: Seasonal variation in nutrients, pelagic primary  
603 production and grazing in a high-Arctic coastal marine ecosystem, Young Sound, Northeast  
604 Greenland, *Mar Ecol Prog Ser*, 179, 13-25, Doi 10.3354/Meps179013, 1999.

605 Sabine, C. L., Feely, R. A., Gruber, N., Key, R. M., Lee, K., Bullister, J. L., Wanninkhof, R.,  
606 Wong, C. S., Wallace, D. W. R., Tilbrook, B., Millero, F. J., Peng, T. H., Kozyr, A., Ono, T., and  
607 Rios, A. F.: The oceanic sink for anthropogenic CO<sub>2</sub>, *Science*, 305, 367-371, 2004.

608 Saros, J. E., Rose, K. C., Clow, D. W., Stephens, V. C., Nurse, A. B., Arnett, H. A., Stone, J. R.,  
609 Williamson, C. E., and Wolfe, A. P.: Melting Alpine Glaciers Enrich High-Elevation Lakes with  
610 Reactive Nitrogen, *Environ Sci Technol*, 44, 4891-4896, 10.1021/es100147j, 2010.

611 Simpson, M. J. R., Milne, G. A., Huybrechts, P., and Long, A. J.: Calibrating a glaciological  
612 model of the Greenland ice sheet from the Last Glacial Maximum to present-day using field  
613 observations of relative sea level and ice extent, *Quaternary Science Reviews*, 28, 1631-1657,  
614 2009.

615 Smith Jr., K. L., A.D., S., T.J., S., and J., S.: Icebergs as Unique Lagrangian Ecosystems in Polar  
616 Seas, *Annual Review of Marine Science*, 5, 269-287, doi:10.1146/annurev-marine-121211-  
617 172317, 2013.

618 Smith, S. L., Smith, W. O., Codispoti, L. A., and Wilson, D. L.: Biological Observations in the  
619 Marginal Ice-Zone of the East Greenland Sea, *J Mar Res*, 43, 693-717, 1985.

620 Stibal, M., Telling, J., Cook, J., Mak, K. M., Hodson, A., and Anesio, A. M.: Environmental  
621 Controls on Microbial Abundance and Activity on the Greenland Ice Sheet: A Multivariate  
622 Analysis Approach, *Microb Ecol*, 63, 74-84, DOI 10.1007/s00248-011-9935-3, 2012.

623 Syvitski, J. P. M., Stein, A. B., Andrews, J. T., and Milliman, J. D.: Icebergs and the sea floor of  
624 the East Greenland (Kangerlussuaq) continental margin, *Arct Antarct Alp Res*, 33, 52-61, Doi  
625 10.2307/1552277, 2001.

626 Tedesco, M., Fettweis, X., Mote, T., Wahr, J., Alexander, P., Box, J. E., and Wouters, B.:  
627 Evidence and analysis of 2012 Greenland records from spaceborne observations, a regional  
628 climate model and reanalysis data, *Cryosphere*, 7, 615-630, DOI 10.5194/tc-7-615-2013, 2013.

629 Tedstone, A. J., Nienow, P. W., Sole, A. J., Mair, D. W. F., Cowton, T. R., Bartholomew, I. D.,  
630 and King, M. A.: Greenland ice sheet motion insensitive to exceptional meltwater forcing,  
631 *Proceedings of the National Academy of Sciences*, 110, 19719-19724,  
632 10.1073/pnas.1315843110, 2013.

633 Telling, J., Anesio, A. M., Tranter, M., Irvine-Fynn, T., Hodson, A., Butler, C., and Wadham, J.:  
634 Nitrogen fixation on Arctic glaciers, Svalbard, *J Geophys Res-Biogeophys*, 116, Artn G03039  
635 Doi 10.1029/2010jg001632, 2011.

636 Telling, J., Stibal, M., Anesio, A. M., Tranter, M., Nias, I., Cook, J., Bellas, C., Lis, G.,  
637 Wadham, J. L., Sole, A., Nienow, P., and Hodson, A.: Microbial nitrogen cycling on the  
638 Greenland Ice Sheet, *Biogeosciences*, 9, 2431-2442, DOI 10.5194/bg-9-2431-2012, 2012.

639 Telling, J., Boyd, E. S., Bone, N., Jones, E. L., Tranter, M., MacFarlane, J. W., Martin, P. G.,  
640 Wadham, J. L., Lamarche-Gagnon, G., Skidmore, M. L., Hamilton, T. L., Hill, E., Jackson, M.,

641 and Hodgson, D. A.: Rock comminution as a source of hydrogen for subglacial ecosystems,  
642 Nature Geosci, 8, 851-855, 10.1038/ngeo2533  
643 <http://www.nature.com/ngeo/journal/v8/n11/abs/ngeo2533.html - supplementary-information>, 2015.  
644 Tranter, M., Brown, G. H., and Sharp, M. J.: The Use of Sulfate as a Tracer for the Delayed  
645 Flow Component of Alpine Glacial Runoff, Tracers in Hydrology, 89-98  
646 350, 1993.  
647 Vancoppenolle, M., Bopp, L., Madec, G., Dunne, J., Ilyina, T., Halloran, P. R., and Steiner, N.:  
648 Future Arctic Ocean primary productivity from CMIP5 simulations: Uncertain outcome, but  
649 consistent mechanisms, Global Biogeochem Cy, n/a-n/a, 10.1002/gbc.20055, 2013.  
650 Vernon, C. L., Bamber, J. L., Box, J. E., van den Broeke, M. R., Fettweis, X., Hanna, E., and  
651 Huybrechts, P.: Surface mass balance model intercomparison for the Greenland ice sheet,  
652 Cryosphere, 7, 599-614, DOI 10.5194/tc-7-599-2013, 2013.  
653 Wadham, J. L., Tranter, M., Skidmore, M., Hodson, A. J., Priscu, J., Lyons, W. B., Sharp, M.,  
654 Wynn, P., and Jackson, M.: Biogeochemical weathering under ice: Size matters, Global  
655 Biogeochem. Cycles, 24, GB3025, 10.1029/2009gb003688, 2010.  
656 Wolff, E. W.: Ice sheets and nitrogen, Philos T R Soc B, 368, Artn 20130127  
657 Doi 10.1098/Rstb.2013.0127, 2013.  
658 Wynn, P. M., Hodson, A. J., Heaton, T. H. E., and Chenery, S. R.: Nitrate production beneath a  
659 High Arctic Glacier, Svalbard, Chem Geol, 244, 88-102, DOI 10.1016/j.chemgeo.2007.06.008,  
660 2007.

661  
662  
663

## 664 **6 Acknowledgments**

665 This research is part of the UK Natural Environment Research Council, NERC funded DELVE  
666 project (NERC grant NE/I008845/1). It was also funded by NERC grants NE/E004016/1 (to J. L.  
667 Wadham), NE/F0213991 to (P.W. Nienow) and a NERC CASE studentship to E. C. Lawson  
668 (NERC DTG/GEOG SN1316.6525) co-sponsored by Dionex Corporation (part of Thermo  
669 Fisher Scientific) and a NERC PhD studentship to J. Hawkings. A. Tedstone was funded by a  
670 NERC studentship and MOSS scholarship. P.W. Nienow was supported by grants from the  
671 Carnegie Trust for University of Scotland and The University of Edinburgh Development Trust.  
672 Additional support was provided by the Leverhulme Trust, via a Leverhulme research fellowship  
673 to J.L. Wadham. We thank all of those assisted with fieldwork at LG, and to Dr Fanny Monteiro

674 who provided comments on an earlier draft. The work was also supported by the Cabot Institute  
 675 at the University of Bristol.

676

677

678

679

680

681

## 682 7 Tables

683 **Table 1** Mean concentrations of nitrogen species reported in LG runoff (including discharge  
 684 weighted mean, DWM for TDN species), in comparison to those in moulin waters, surface ice  
 685 (pre-melt and post-melt “Summer ice”, where the latter samples were at the melting temperature  
 686 and contained dispersed debris), snow, cryoconite water and basal ice (a-(Telling et al., 2012), b-  
 687 (Wolff, 2013))

	NO <sub>3</sub> <sup>-</sup> (μM)			NH <sub>4</sub> <sup>+</sup> (μM)			DIN (μM)			DON (μM)			TDN (μM)		
	mean	SD	n	mean	SD	n	mean	SD	n	mean	SD	n	mean	SD	n
Bulk runoff-dissolved	1.8	1.2	62	0.4	0.6	62	2.2	1.4	62	2.3	1.5	62	4.5	2.3	62
Bulk runoff-dissolved, DWM	1.1	-	-	0.3	-	-	1.4	-	-	1.7	-	-	3.2	-	-
Bulk runoff-sediment bound	n.d.	n.d.	-	1.2	0.6	39	1.2	n.d.	-	n.d.	n.d.	-	1.2	n.d.	-
Bulk runoff-sediment bound DWM	n.d.	n.d.	-	1.4	-	39	n.d.	n.d.	-	n.d.	n.d.	-	n.d.	n.d.	-
Moulins (same time period)	0.7	1.4	28	0.6	0.5	28	2.0	1.2	28	1.1	1.3	28	2.2	1.4	28
<b>SURFACE</b>															
Pre-melt ice <sup>a</sup>	0.59	0.14	6	0.3	0.1	6	0.9	0.3	6	0.0	0.0	6	0.6	0.1	6
Snow <sup>a</sup>	1.03	0.17	3	0.45	0.0	3	1.1	0.2	3	0.0	0.0	3	1.02	0.14	3
GriS ice cores <sup>b</sup>	0.97	n.d.	-	0.45	n.d.	-	1.4	n.d.	-	n.d.	n.d.	-	n.d.	n.d.	-
Summer ice	0.64	0.42	7	0.6	0.6	7	1.3	0.9	7	3.0	2.6	7	2.9	2.1	7
Cryoconite meltwater	1.4	0.4	6	1.1	1.3	6	1.7	0.9	6	0.7	0.4	6	2.4	1.1	6
<b>SUBGLACIAL</b>															
Basal ice	1.5	0.0	6	2.7	0.1	6	3.7	0.1	6	12	1.3	6	15	1.3	6
Incubations (aerobic)	1.4	2.1	7	2.5	2.2	7	3.9	2.5	7	3.36	2	7	7.1	1.7	7
Incubations (anaerobic)	1.03	1.4	6	0.76	0.2	6	1.8	1.3	6	1.79	1	6	5.3	1.4	6

688

689

690

691

692 **Table 2** Estimates of seasonal fluxes of total dissolved (TDN) and particulate nitrogen (SS-  
693  $\text{NH}_4^+$ ) species (total nitrogen=TN) from Leverett Glacier and the Greenland Ice Sheet in 2000-  
694 2010 and 2012 (values marked with an asterisk were below the analytical limit of detection but  
695 and hence, are purely indicative)

<b>Glacial Runoff: Leverett Glacier (LG)</b>							
<sup>b</sup> LG Water Flux ( $\text{km}^3 \text{a}^{-1}$ ) (2012)	2.2						
Concentration LG ( $\mu\text{M}$ )	TDN	DIN	DON	$\text{NO}_3^- \text{-N}$	$\text{NH}_4^+ \text{-N}$	$\text{SS-NH}_4^+ \text{-N}$	TN+SS-NH4+
min	0.9*	0.5	0.1	0.1	0.4*	*0.31	1.2
DWM	3.2	1.5	1.7	1.1	0.3	1.4	4.6
max	11	7.5	6.3	5.1	2.4	3.7	15
Flux LG ( $\text{t a}^{-1}$ ): 2012	TDN	DIN	DON	$\text{NO}_3^- \text{-N}$	$\text{NH}_4^+ \text{-N}$	$\text{SS-NH}_4^+ \text{-N}$	TN+SS-NH4+
min	28	15	3	3	12	10	37
DWM	99	46	52	34	9	43	142
max	339	231	194	157	74	114	453
Yield, using DWM ( $\text{kg N km}^2 \text{a}^{-1}$ )	164	77	87	56	15	72	236

696 <sup>b</sup>-measured water flux from Leverett Glacier (this manuscript)

697 **Table 3** Estimates of seasonal fluxes of total dissolved (TDN) and particulate nitrogen (SS- $\text{NH}_4^+$ )  
698 species (total nitrogen=TN) from the Greenland Ice Sheet in 2000-2010 and 2012

<b>Glacial Runoff: Greenland Ice Sheet</b>							
<sup>a</sup> GrIS Water Flux ( $\text{km}^3 \text{a}^{-1}$ ) (2000-2011)	418						
<sup>a</sup> GrIS Water Flux ( $\text{km}^3 \text{a}^{-1}$ ) (2012)	665						
	TDN	DIN	DON	$\text{NO}_3^- \text{-N}$	$\text{NH}_4^+ \text{-N}$	$\text{SS-NH}_4^+ \text{-N}$	TN+SS-NH4+
<b>Flux GrIS (<math>\text{Gg a}^{-1}</math>): 2000-2010</b>							
Min	5.3	3	1	1	2	2	7.1
DWM	19	9	10	6	2	8	27
Max	64	44	37	30	14	22	86
<b>Flux GrIS (<math>\text{Gg a}^{-1}</math>): 2012</b>							
Min	8.4	4.7	0.9	0.9	3.7	2.9	11
DWM	30	14	16	10	2.8	13	43
Max	102	70	59	47	22	34	137
<b>Ice Discharge Greenland Ice Sheet</b>							
<sup>a</sup> GrIS Iceberg Discharge ( $\text{km}^3 \text{a}^{-1}$ )	~600						
	TDN	DIN	DON	$\text{NO}_3^- \text{-N}$	$\text{NH}_4^+ \text{-N}$	$\text{SS-NH}_4^+ \text{-N}$	TN+SS-NH4+
	1.4	1.4	0	0.97	0.45	n/a	1.4
	12	12	0.0	8	4	n/a	12
<b>Arctic River Discharge</b>							
<sup>c</sup> Arctic River mean summer water flux ( $\text{km}^3 \text{a}^{-1}$ )	169						
	TDN	DIN	DON	$\text{NO}_3^- \text{-N}$	$\text{NH}_4^+ \text{-N}$	$\text{SS-NH}_4^+ \text{-N}$	TN+SS-NH4+
<sup>c</sup> Concentration Arctic Rivers ( $\mu\text{M}$ )	14	2.7	12	2.0	0.7	n/a	n.d.
<sup>d</sup> Mean summer flux Arctic Rivers ( $\text{Gg a}^{-1}$ )	41	8.8	33	7.7	<0.5	n.d.	n.d.

699



700

## 701 8 Figure Captions

702 **Figure 1** Map showing the study area, including the location of Leverett Glacier runoff sampling  
703 station (white dot), surface sampling site (red dot) and the basal ice sampling location (brown  
704 dot), together with Søndre Strømfjord and the Watson River, into which runoff from Leverett  
705 Glacier drains.

706 **Figure 2 Times series of nitrogen species in LG runoff from the 2012 melt season** depicting  
707 concentrations of a) bulk meltwater suspended sediment and sediment-bound ammonium (SS-  
708  $\text{NH}_4^+$ ) b) TDN and DON, c) dissolved nitrate and ammonium, and instantaneous fluxes of, d)  
709  $\text{SS-NH}_4^+$  (bulk meltwater discharge,  $Q$ , is also shown), e) TDN and DON and f) dissolved nitrate  
710 and ammonium. Vertical dotted lines (left to right) indicate 1<sup>st</sup> May, 1<sup>st</sup> June and 1<sup>st</sup> July, 2012.  
711 The grey shaded bars reflect inferred subglacial outburst events (Hawkings et al., 2014)

712 **Figure 3 Associations between TDN and DIN** in a) runoff, moulin waters, snow and pre-melt  
713 ice, where data on snow and pre-melt ice are from (Wolff, 2013; Telling et al., 2012) and b)  
714 runoff and glacier surface ecosystems (cryoconite holes, summer ice including dispersed debris)  
715 and subglacial ecosystems (basal ice and meltwaters sampled from anaerobic/aerobic long-term  
716 subglacial (SG) incubation experiments). A line indicates ratios of 1 for TDN/DIN where the  
717 TDN content of samples is entirely comprised of DIN. Samples that plot below this line have a  
718 dissolved organic nitrogen component. All samples have been blank corrected and error bars  
719 reflect the uncertainty of nutrient analyses given known precision and accuracy.

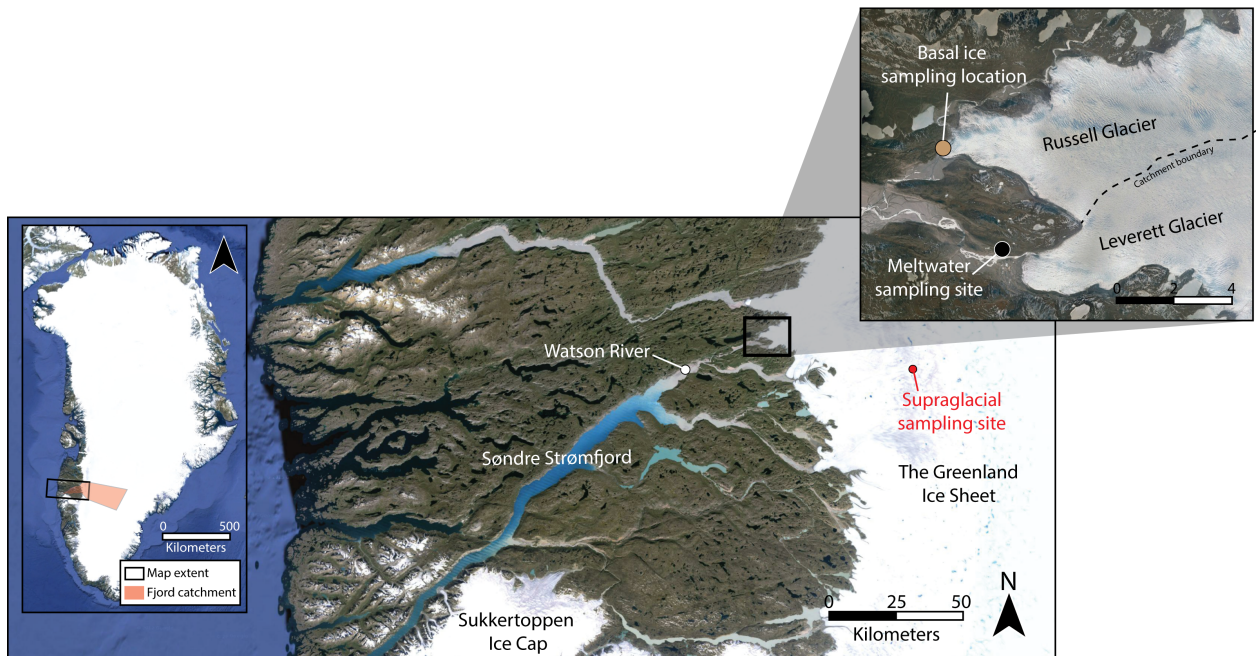
720 **Figure 4** Association between the TDN concentrations measured simultaneously at the moulin  
721 and runoff monitoring sites (the correlation is significant at the 99% confidence level). Insets  
722 show the same data (excluding runoff samples) at low concentrations ( $< 6 \mu\text{M}$ ).

723 **Figure 5** Time series of dissolved nitrogen concentrations measured in a) Live aerobic, b) Live  
724 anaerobic c) Sediment-free aerobic and d) Sediment-free anaerobic incubation experiments (note  
725 the difference in scale for the y axis between a) and b)-d).

726 **Figure 6** Times series of a) bulk discharge, b) concentrations of sediment-bound  $\text{NH}_4^+$  ( $\text{P-NH}_4^+$ )  
727 and dissolved sulphate and c) concentrations of DON and dissolved  $\text{NH}_4^+$  in runoff measured  
728 during the first (and main) subglacial outburst event during the 2012 season.

729 **Figure 1**

730



731

732

733

734

735

736

737

738

739

740

741

742

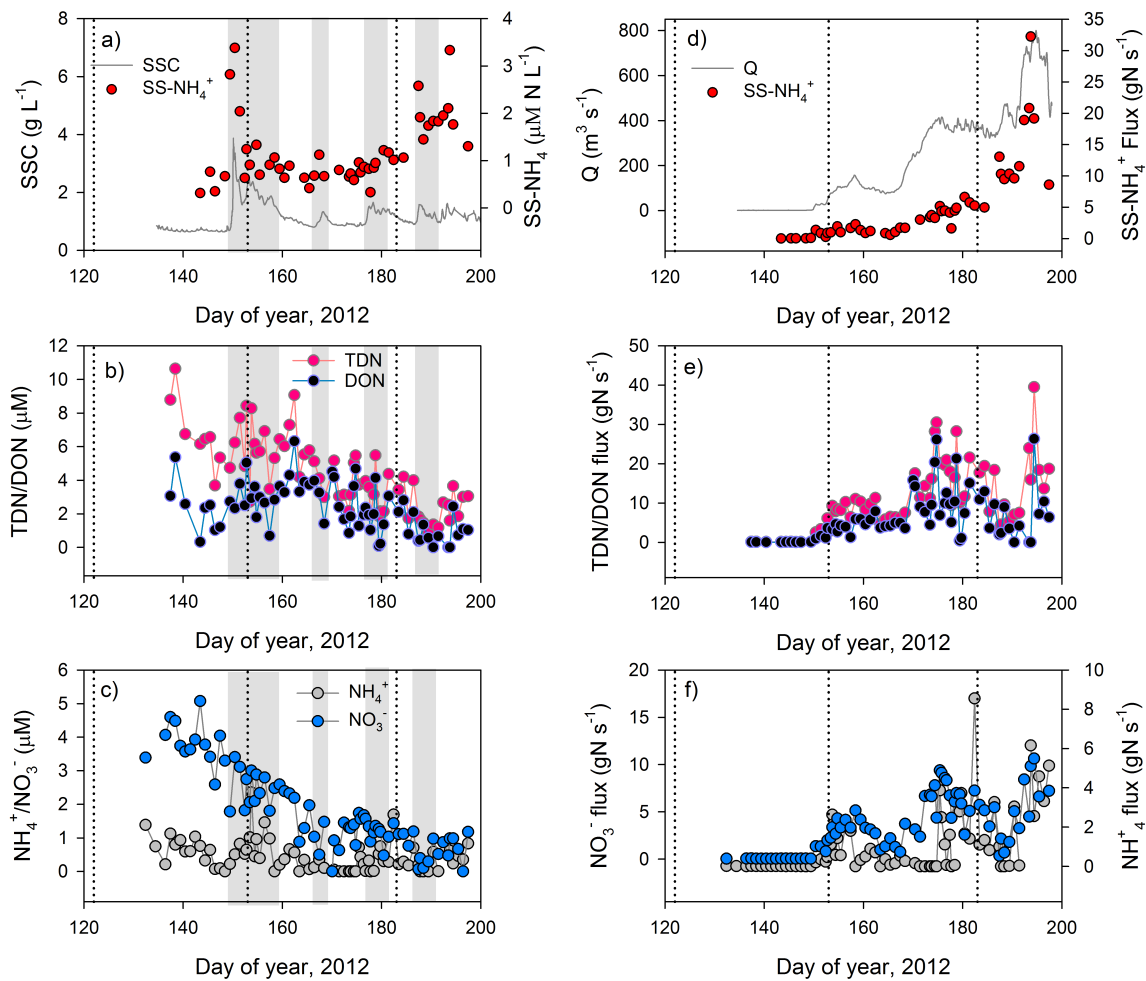
743

744

745

746

Figure 2



747

748

749

750

751

752

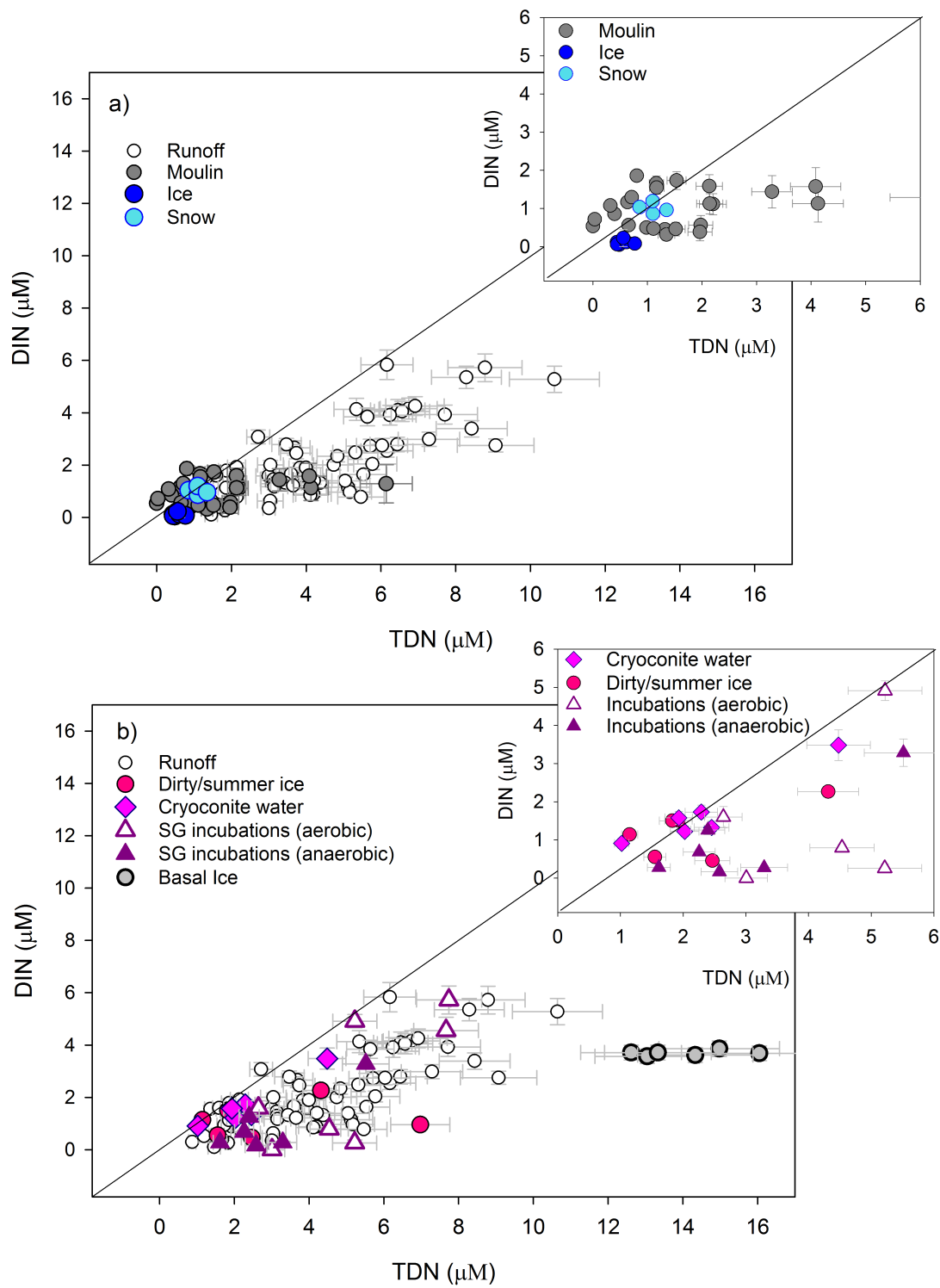
753

754

755

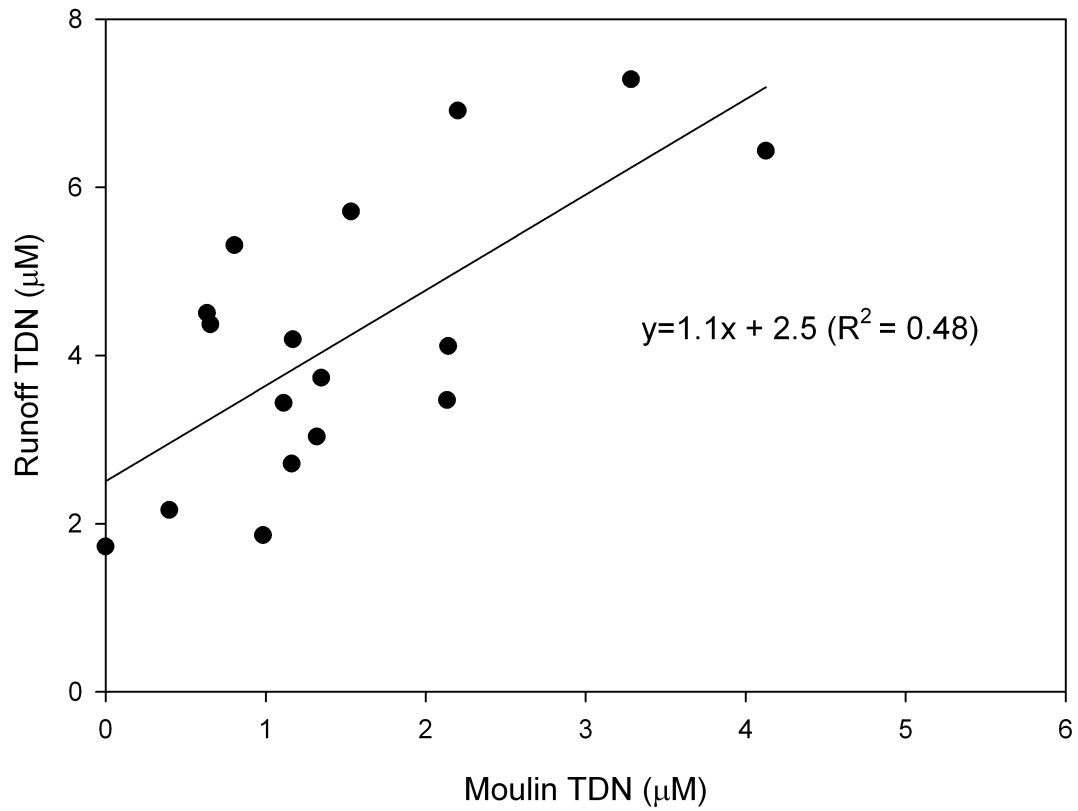
756

757



761

762 **Figure 4**



763

764

765

766

767

768

769

770

771

772

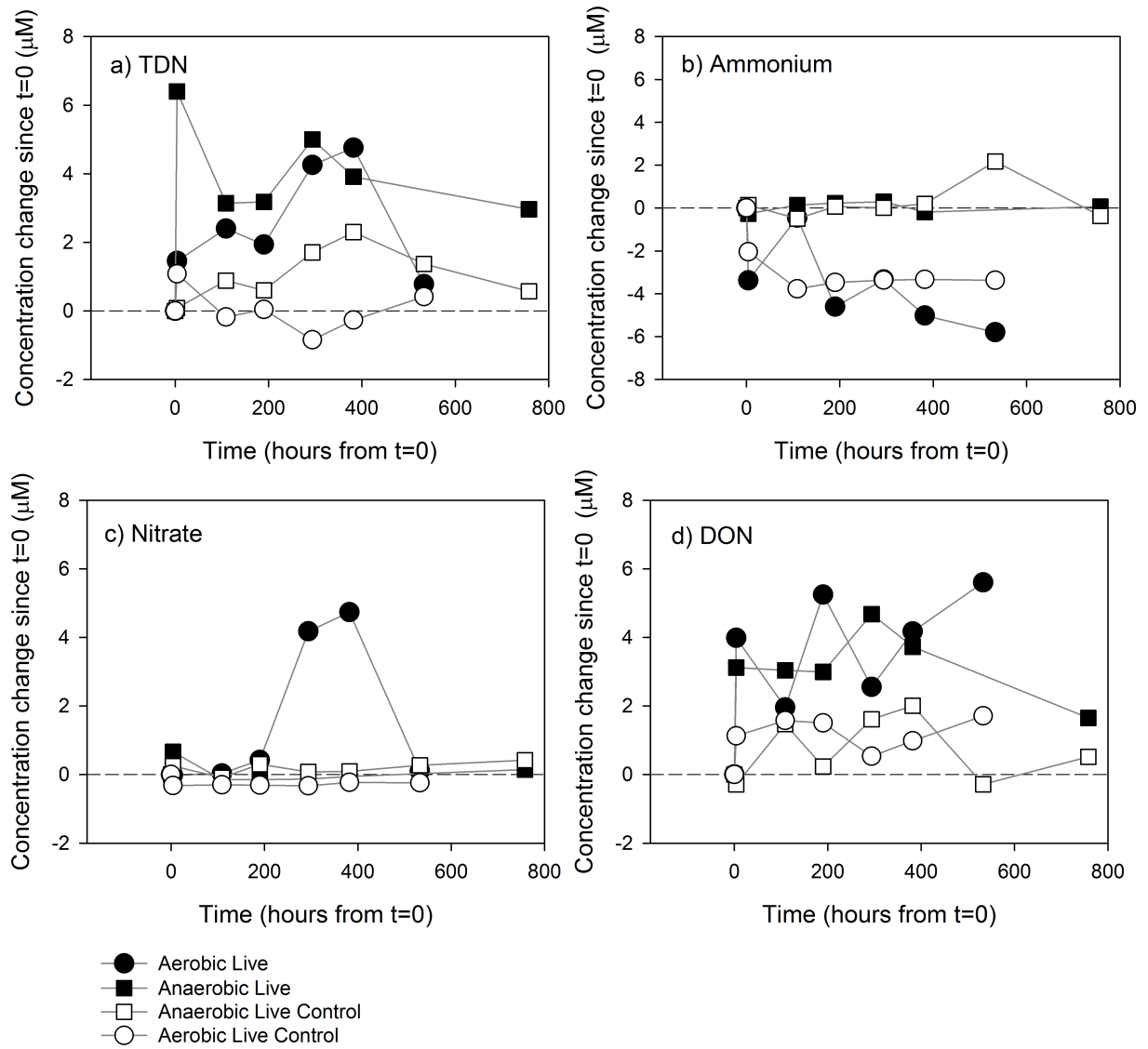
773

774

775

776

Figure 5



778

779

780

781

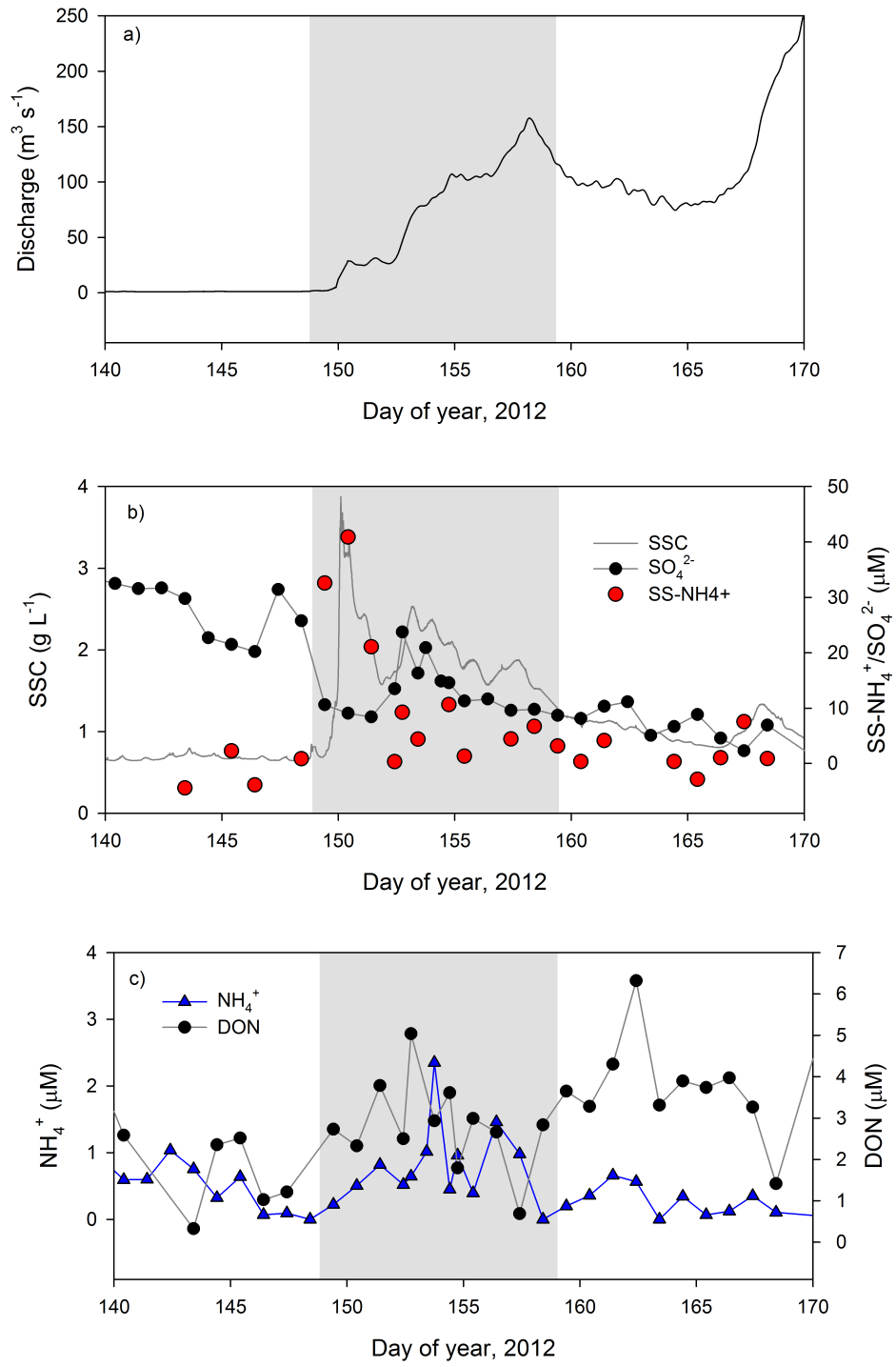
782

783

784

785

786



790

791

792